Observation of individual macroscopic quantum tunneling events in superconducting nanowires

Meenakshi Singh and Moses H. W. Chan
The Center for Nanoscale Science and Department of Physics, The Pennsylvania State University, University Park, Pennsylvania 16802-6300, USA

(Received 24 October 2012; revised manuscript received 4 August 2013; published 26 August 2013)

In quasi-one-dimensional nanowires, superconductivity is destroyed by phase slip events. Phase slips can be caused by thermal activation over a free energy barrier (TAPS) or quantum tunneling through the barrier (QPS). Quantum phase slip is an example of macroscopic quantum tunneling. Here, we report the observation of QPS experimentally separated from interference of TAPS in aluminum nanowires. This separation between the low-temperature QPS and the high-temperature TAPS regions is made possible by a phase slip free superconducting region stabilized by the dissipative environment viz. the normal electrodes. Individual QPSs are detected by means of a single-shot voltage measurement protocol, in which they appear as stochastic switching events from the superconducting to the normal state.

DOI: 10.1103/PhysRevB.88.064511 PACS number(s): 74.45.+c, 74.40.Kb, 74.78.−w

I. INTRODUCTION

Superconductivity is characterized by a macroscopic wave function $|\psi(r)|\,e^{i\varphi(r)}$, often thought of as an order parameter. In a bulk system, the amplitude and phase coherence vanish simultaneously at the superconducting transition temperature. This is not the case in two-dimensional (2D) and quasi-one-dimensional (1D) systems. In a nanowire in the 1D limit, i.e. when it is thinner than the superconducting coherence length, phase coherence along the wire can vanish through phase slips.[1] In a phase slip event, ψ reduces to zero at some point along the wire. Such events cause resistance to appear momentarily for an interval $\tau_{GL} \sim 10^{-12}$ s (the Ginzburg-Landau relaxation time). A phase slip can be thermally activated (TAPS),[2–5] which takes the system over a free energy barrier (ΔF). The height of ΔF depends on several parameters, like the critical field and the cross-sectional area of the wire, and is a rapidly decreasing function of the applied current (I). The probability of TAPS scales as $e^{-\frac{\Delta F}{k_B T}}$, making these events extremely improbable at temperatures well below T_c and increasingly likely as the temperature rises towards T_c. The system can also go across the barrier via quantum tunneling, known as quantum phase slips (QPS). Quantum phase slips can occur at temperatures well below T_c ($P \propto e^{-\frac{\Delta F}{\hbar\omega_0}}$, where $\hbar\omega_0$ is some energy). These phase slips are examples of macroscopic quantum tunneling (MQT) because the collective state of a large number of electrons is involved.[6] Macroscopic quantum tunneling has been experimentally observed in Josephson junctions[7–10] and the corresponding theoretical foundations developed a while ago.[11,12] It was also recently observed in a superconducting loop.[13] While a single superconducting nanowire is arguably the simplest system to observe QPS, yet despite theoretical predictions[14–16] and intense experimental efforts, evidence of QPS in superconducting nanowires remain sparse.[17–27] The major challenge associated with the study of QPS in nanowires is the differentiation between classical TAPS and quantum tunneling events. In a number of previous experiments, fitting with multiple parameters was used to demonstrate the possible existence of QPS at temperature far below the transition temperature.[17–22] This demonstration hinges on the broadening of the superconducting transition relative to expectations from the TAPS. As noted by other papers, there are potential pitfalls in interpreting the data via these fitting procedures.[18,23,24,28] In an actual experimental situation, the Joule heating associated with a finite measurement current complicates the quantitative fitting and interpretation. In fact, at high currents, not only does the probability of a phase slip (both TAPS and QPS) increase, the heating from a single phase slip event can cause the entire system to turn normal.[29–31] Such a possibility becomes especially relevant at low temperatures, where the dissipation of the Joule heating due to the measurement current is not efficient. In addition to the Joule heating effect, several other effects have been suggested to cause additional (compared to pure TAPS) broadening of the resistive transition, e.g. 1D Coulomb correlation effects[22] and inhomogeneities of the wire.[23] An approach to study QPS was adopted in a recent experiment in which the current at which the nanowire switched from the superconducting to the normal state was recorded as a function of bath temperature.[24] The switching rate was calculated and could not be explained on the basis of the TAPS model alone, as it saturates at low temperatures. Existing QPS models were used to fit the high switching rates at low temperatures. This approach of saturation of switching current distribution has been used in several experiments since to demonstrate QPS.[8,9,27] Our experiment offers a way to study QPS free from interference from TAPS. In this paper, we describe a nanowire system where TAPS and QPS regimes are clearly separated by a stable superconducting region and can be qualitatively differentiated. This separation is made possible by the antiproximity effect (APE),[32–36] an experimental realization of the Caldeira-Leggett model.[37–40] In the Caldeira-Leggett model, the probability of quantum tunneling is exponentially suppressed by coupling to a dissipative environment. This coupling can therefore be used to turn the QPS events on or off.[41,42]

II. SAMPLE SYNTHESIS AND CHARACTERIZATION

Aluminum nanowires (AlNWs) with widths (w) ranging from 50–150 nm and thickness (d) = 50 nm were synthesized using standard e-beam lithography process with patterning on a MAA/PMMA bilayer followed by e-beam-assisted evaporation of Al at 0.5 Å/s. We found that changes in the evaporation rate and the vacuum level in the evaporator

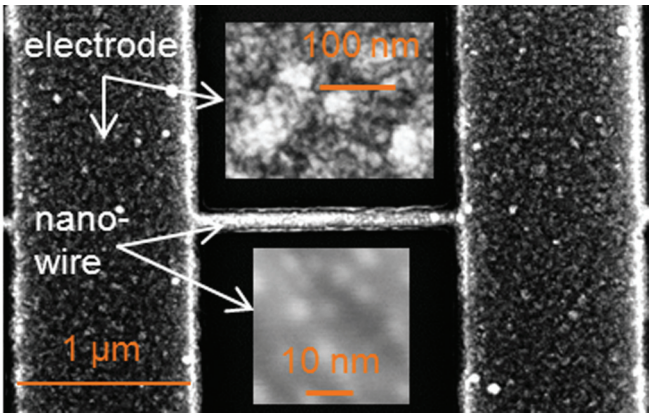

FIG. 1. (Color online) Scanning electron micrograph of an AlNW (120 nm wide, 50 nm thick) and the electrodes (1 micron wide, 50 nm thick).

while evaporating the Al can change the grain size and the impurity level, thereby affecting the superconducting critical temperature (T_c) of the Al.[43] The substrate is lightly n-doped Si wafer with a 120-nm-thick insulating layer of Si_3N_4 grown by low-pressure chemical vapor deposition (LPCVD).

Figure 1 shows a scanning electron micrograph (SEM) of an AlNW and its electrodes. The wire and electrodes were evaporated simultaneously using a single mask, ensuring excellent electrical contact. The nanowire and the electrodes are both granular. However, the grain size in the electrodes (top inset) is much larger than the grain size in the AlNW (bottom inset). This may be a consequence of the lateral confinement in the nanowire region during evaporation. This effect has also been studied using SEM in evaporated Zn nanowires, where the grain size in the nanowires was found to be of the order of the wire diameter.[35] The difference in grain size is important for our experiment since the T_c and H_c of the superconductor are known to depend on the grain size.[43] The electrodes and nanowires in our experiment, therefore, have different T_c and H_c (see Fig. 2). The T_c and the H_c of the nanowire ($\sim$1.4 K and 4000 Oe) are much higher than bulk Al. The T_c and H_c of the electrodes ($\sim$1.0 K and 300 Oe), on the other hand, are very close to bulk.

The resistivities of the samples fabricated in this manner are found to range from 5.41×10^{-8} Ω-m to 2.22×10^{-6} Ω-m. The T_c and H_c of samples with higher resistivity are higher. It is important to note here that the resistivities of all the samples we have studied put them in the regime where all grains are in good metallic contact with each other and cannot be thought of as arrays of Josephson junctions.[44] A total of 10 such samples were studied, and stochastic switching triggered by individual QPS was found in five. In general, the wires with the lowest electrical resistivity did not show switching behavior (Fig. S4).[45] In accordance with the Wiedemann-Franz Law, these are also the samples with the highest thermal conductivity. So, the samples that are most efficient at dissipating heat, do not show the switching behavior. Calculations showing that the difference between the samples with and without switching is rooted in how efficiently the heat pulse due to QPS is dissipated from the wire are included in the Supplemental Material.[45] In the main text of this paper, we feature data from samples 1 and 2. The results from samples 3, 4, and 5 are completely consistent with these. Both samples 1 and 2 have a 5-nm-thick Au protective layer on the Al nanowire. There are no qualitative differences between the samples with and without this protective layer.

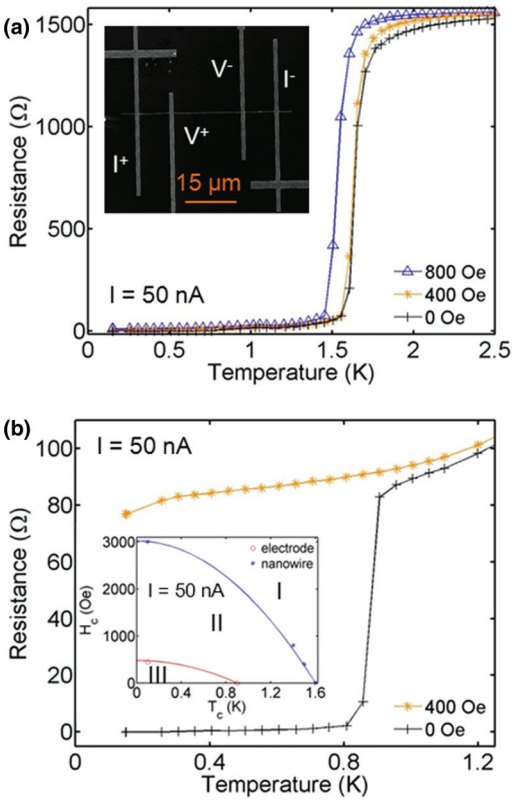

FIG. 2. (Color online) Standard transport measurements of a 100-nm-wide, 50-nm-thick, 20-μm-long AlNW (sample 1) showing no QPS at 50 nA. (a) Resistance as a function of temperature at different fields. The inset shows an SEM of the AlNW and the four Al electrodes. (b) Resistance as a function of temperature for one of the Al electrodes obtained from a three-electrode measurement of the same sample. The inset shows a schematic phase diagram. The points are experimentally measured critical fields, and the solid lines represent the empirical relation $H_c(T) = H_c(0)[1 - (T/T_c)^2]$ plotted using experimentally determined T_c and $H_c(0)$ as a free parameter.

III. EXPERIMENTAL SETUP

The measurements reported in this paper are performed in a dilution refrigerator (DR) with a base temperature of 50 mK inserted into a Quantum Design Physical Property Measurement System (PPMS). The system is equipped with a 9-T magnetic field. The sample, i.e. the Si substrate with the AlNW, is glued to the sample puck of the PPMS by means of GE varnish. The sample puck is a plug-in sample mount with eight pins that connect to the DR electronics (provided by Quantum Design). The sample puck is mechanically and thermally anchored to the mixing chamber of the dilution refrigerator. The Joule heating due to the measurement current flowing in the AlNW when the nanowire is in the normal state or when it is going through a phase slip is drained to the sample puck through two parallel channels. Heat is conducted from the

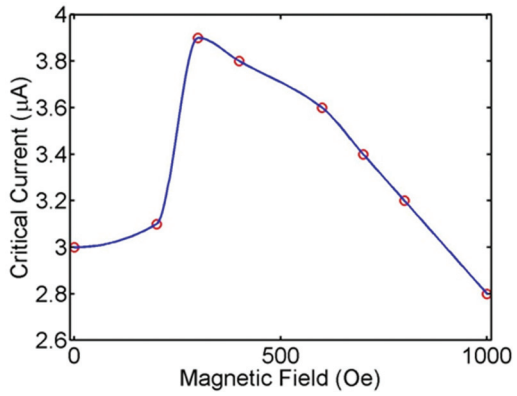

FIG. 3. (Color online) Transport measurements showing the evolution of critical current I_c with applied field, I_c as a function of applied field for sample 1. Instead of decreasing with field as expected, the critical current increases, peaking at the critical field of the electrodes. On further increasing the applied field, it decreases in accordance with conventional expectations. The open circles are the data points and the solid line is a guide to the eye.

AlNW through the substrate and the GE varnish to the sample puck and also through the four thin (0.075-mm diameter) gold wires pressed onto the electrodes pads that are heat sunk to the sample puck. Due to the large Kapitza thermal boundary resistance at the AlNW-Si-wafer and Si-wafer-sample-puck interfaces, the thermal path through the gold wires is far more efficient. We show in the Supplemental Material[45] that this is particularly true for AlNW of low resistivity. The resolution of the electrical measurements is ∼20 nV (user bridge supplied by Quantum Design). All electrical leads are equipped with low-pass Pi filters at room temperature.

IV. RESULTS AND ANALYSIS

An AlNW with 4 Al electrodes patterned on it for electrical measurement is shown in the inset of Fig. 2(a). Figure 2(a) shows the R-T plots at different applied fields (H) perpendicular to the plane of sample 1. The superconducting transition is rounded, and zero resistance—defined by the instrumental resolution of 20 nV—is found below $T = 0.8$ K. This indicates that TAPS[2,3] freeze out near T_c, and the probability of QPS is so low at this excitation current ($I = 50$ nA) that a superconducting state exists at low temperatures. This is the expected R-T behavior in relatively wide nanowires at low excitation currents.[21,46] Here, R-T of one of the electrodes (obtained by including it in the measurement) is shown in Fig. 2(b). The T_c and H_c of the electrode are lower than that of the AlNW. The difference in grain size is likely to be responsible for the differences in critical temperatures and fields between the AlNW and the electrodes. This grain size dependence of the superconductivity of Al is well known experimentally[43,47] and has also been analyzed theoretically.[48]

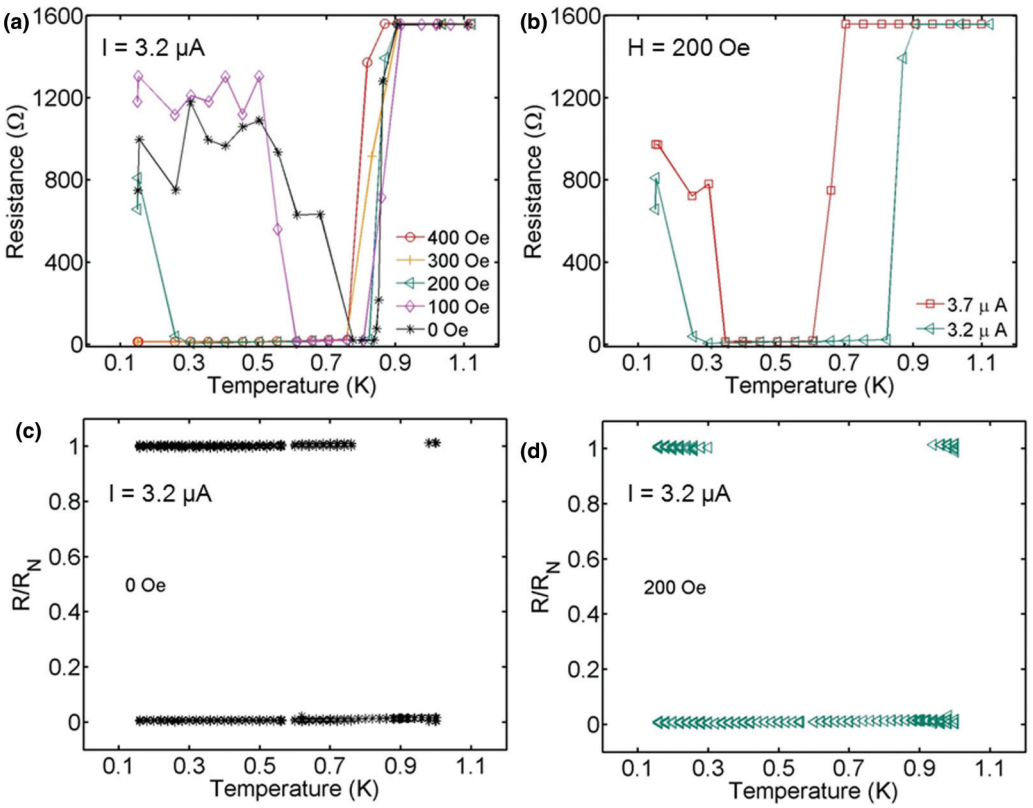

FIG. 4. (Color online) Transport measurements showing the antiproximity effect and QPS in sample 1. (a) Resistance as a function of temperature at different fields at 3.2 μA. (b)Resistance as a function of temperature at 200 Oe field at 3.2 and 3.7 μA. (c) and (d) Normalized resistance (R/R_N where $R_N \sim 1554\ \Omega$) from single-shot measurements as a function of temperature measured at 3.2 μA and applied fields of 0 and 200 Oe, respectively. The nonzero resistance at low temperature is a consequence of QPS. Individual QPS are revealed by single-shot measurements [panels (c) and (d)].

A schematic phase diagram at $I = 50$ nA is shown [inset of Fig. 2(b)]. In region I, both the AlNW and the Al electrodes are normal. In region II, the electrodes are normal, and the AlNW is superconducting; and in region III, the electrodes and AlNW are both superconducting. On increasing I, the phase boundary for the AlNW moves towards lower H and T, whereas the phase boundary for the electrodes stays nearly unchanged, narrowing region II.

In Fig. 3, we present the evolution of critical current (I_c) of sample 1 with applied magnetic field. According to conventional expectations, the I_c should decrease on the application of a magnetic field. In these samples, however, on increasing the applied magnetic field, the I_c increases, peaks at the critical field of the electrodes, and then decreases. This unconventional dependence of the I_c on applied magnetic field is a signature of the APE and has been seen before in Zn and electrochemically synthesized Al nanowires.[32–36] The APE is different from an anomalous negative magnetoresistance also seen in superconducting structures,[49,50] as it has also been seen in the absence of a magnetic field.[36] The difference from a theoretical perspective is discussed by Vodolazov.[51] It is believed that the APE is caused by a proliferation of QPS in the absence of a bulk dissipative environment.[40] To study the sample in this regime, we need to perform measurements at excitation currents falling within the APE peak region of 3.0–3.9 μA shown in Fig. 3. We therefore repeat transport measurements on sample 1 at an excitation current of 3.2 μA.

Under a high excitation current of $I = 3.2$ μA [Fig. 4(a)], sample 1 shows a re-entrant resistive state in region III [see inset of Fig. 2(b)]. This re-entrant state has been observed before in electrochemically synthesized and evaporated Zn nanowires.[32–35] The measured resistance values, in contrast to those in regions I and II, unexpectedly show substantial scatter. This unexpected resistive state can be explained in terms of QPS. While the probability of QPS is extremely small at low currents, as seen in Fig. 2(a), at high currents, both TAPS and QPS become exponentially more likely. In the high-current-measurement regime, therefore, both TAPS and QPS can occur in these relatively thick samples. In addition to the increased probability of phase slips, the heating from a single phase slip at high current can cause the entire system to switch from superconducting to the normal state.[29–31] With this in mind, the high-current results shown in Fig. 4(a) can be understood as follows. At temperatures close to T_c, TAPS are the dominant mechanism for the appearance of the resistive state and lead to the well-known rounding of the superconducting transition. At lower temperatures, in region II, TAPS die out, and the nanowire becomes superconducting. The absence of QPS in this region is explained by the Caldeira-Leggett model, namely quantum tunneling is suppressed by the coupling of the wire to a dissipative environment, the normal electrodes.[37,40] Therefore, region II is too cold for TAPS and protected from QPS by the normal electrodes. In region III, with the electrodes superconducting, QPS occur, and the nanowire becomes resistive. Thus, the classical TAPS process and the quantum QPS process are clearly demarcated. With increasing current, region II becomes narrower, as seen in Fig. 4(b). We now explore the nature of the APE resistive state.

In the results discussed above, each data point corresponds to an average of 50 measurements obtained by applying dc currents of $+I$ and $-I$ alternately, each lasting 0.03 s. Instead of these standard multiple-point averaged measurements, we employed a single-shot procedure. In this procedure, at a given temperature and magnetic field, the resistances were measured for just one cycle comprised of two resistance measurements at dc currents of $+I$ and $-I$. The resulting average resistance from these two measurements was separated into two single resistance readings following the procedure described in the Supplemental Material (Figs. S1 and S2).[45] There was a 10-s interval between each cycle. This method enables us to obtain individual resistance measurements at each value of temperature and field instead of having the averaged

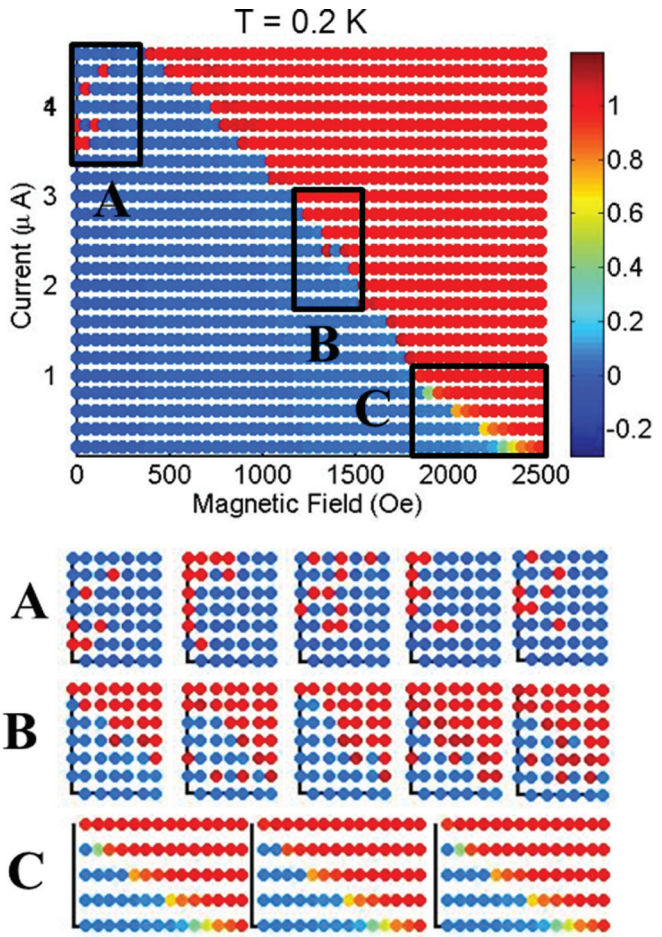

FIG. 5. (Color online) Map of normalized resistance at 0.2 K for a 120-nm-wide, 50-nm-thick, 5-μm-long AlNW (sample 2). (a) Normalized resistance (R/R_N where $R_N \sim 562$ Ω) as a function of applied field and current at 0.2 K obtained using single measurement protocol. To obtain each point, the temperature and magnetic fields were first set to given values, and then the current was ramped up to the required value. Blue corresponds to the superconducting state and red to the normal state. The area marked A is the region where switching between the normal and superconducting states is triggered by quantum phase slips. The area marked B is part of the region where switching is triggered by thermal phase slips. The area marked C is the region where a phase slip does not cause switching. The panels below the figure are a representative sampling of the maps obtained in other scans across the phase space. They feature areas A, B, and C and highlight the stochastic nature of the switching triggered by individual phase slips.

resistance over 50 measurements. Here, 120 such single-shot measurements were made at every value of T and H [Figs. 4(c) and 4(d)]. To reiterate the relationship between the averaged measurements and the single-shot ones, if we numerically average the 120 resistance values at each temperature in Figs. 4(c) and 4(d), we will recover the 0 and 200 Oe traces in Fig. 4(a) (also see Fig. S2 in the Supplemental Material).[45]

Interestingly, the data from these single shot measurements, unlike the averaged measured values shown in panels (a) and (b) are virtually free of scatter. In region II, zero resistance is found in every measurement. At the boundary between regions I and II (near T_c) and in region III (low T), the resistance switches between 0 Ω, (superconducting state) and 1600 Ω (normal state). The resistance in any particular measurement is independent of the previous measurement. The switching near T_c is due to TAPS, while QPSs trigger the switching at low temperature. The averaged measurements shown in Fig. 4(a) reflect the probability of obtaining the normal state in a single measurement at any given temperature. Our data suggests that, if the AlNW does not switch while the current is ramped up to its final value, it does not switch at all. The probability of phase slip, therefore, appears to depend on the rate of current sweep. This dependence, although hinted at,[52] has not been explored in previous studies and is deserving of systematic study in the future. Following the theoretical model of Shah *et al.*,[29,30] we will show that a single QPS event at low temperature in the superconducting nanowire is sufficient to cause a switch to the normal state. Each switching event, therefore, corresponds to a single QPS.

A single phase slip makes a region ($\sim\xi$ in spatial extent) nonsuperconducting for time $\sim 10^{-12}$ s and introduces heat $hI/2e$ into the nanowire. This heat flows along the wire to the superconducting electrodes and also via phonon coupling from the wire to the substrate.[53] The second of these channels is found to be the dominant one for wires showing switching. Following Li *et al.*,[54] a heat flow equation is used to estimate the final temperatures of the nanowire after a single phase slip.[45] The relevant parameters for the heat flow equation are estimated using existing studies on the thermal properties of Al, other metals and metal-semiconductor interfaces.[55–60] At low temperature ($\sim$0.2 K) after a single phase slip, the temperature rises momentarily to $\sim$8.9–13.4 K causing a normal current in the nanowire. Once there is normal current, there is Joule heating, and steady state temperatures between 1.6 and 2.7 K during the measurement time are obtained. Therefore, a single phase slip at low temperatures can easily bring the nanowire to and keep it in the normal state. These calculations are carried out assuming conditions that are skewed for efficient heat dissipation, e.g. the substrate and the electrodes are assumed to be anchored at bath temperature with no additional thermal resistance, and the electrodes are assumed to be normal. Even with these assumptions, a single phase slip in the system results in switching at low temperatures. This analysis is also broadly valid in explaining switching due to the TAPS. However, as T is brought towards T_c, TAPS proliferate, and the switching to the normal state is not necessarily related to a single phase slip. We have carried out detailed field, temperature, and current dependence of the switching phenomenon, and the results are presented below. A map of the normalized resistance of sample 2 at different H and I at 0.2 K obtained by the single measurement protocol is shown in Fig. 5 (the 0.5 K map is shown in Fig. S3 in the Supplemental Material).[45] Measurements were repeated, resulting in 120 such maps. In order to illustrate the stochasticity in the switching phenomenon, the relevant cutout regions from a few of these other maps are shown together with Fig. 5. At low currents and high field, with the electrodes normal, the resistance show a smooth change from zero to the normal state value as a function of current and field (area A) in all the maps. With increasing current, the transition evolves from being continuous to one where the resistance switches discontinuously between the normal and the superconducting states near H_c. The cutouts (area B) show that the switchings, triggered by TAPS, are found at different current and field values in different maps. There is another area showing switching deep in the nanowire's superconducting state where the electrodes are also superconducting (area C in Fig. 5). The switchings here are triggered by QPS and are also random in the H-I phase space.

The probability of finding the nanowire in the normal state in any measurement (P_N) is determined by counting the occurrences of the normal state from the maps [Figs. 6(a) and 6(b)]. As I is increased, the TAPS region moves to lower fields towards the QPS region. At high enough I, the stable superconducting region disappears, and the TAPS and QPS regions merge. Even without any fitting procedures, it is evident that

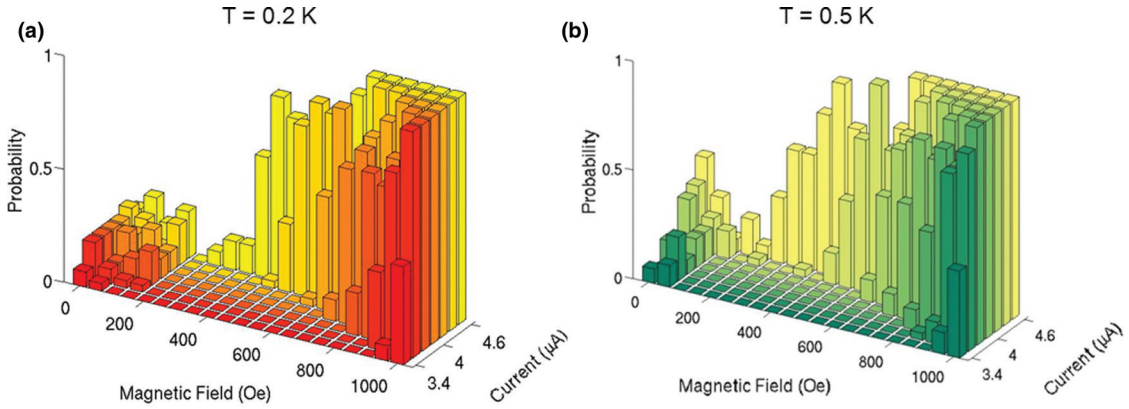

FIG. 6. (Color online) Probability of the normal state at different temperature, field, and current for sample 2. (a) and (b) Probability of finding the normal state in a particular measurement at different fields and currents for temperature 0.2 and 0.5 K, respectively.

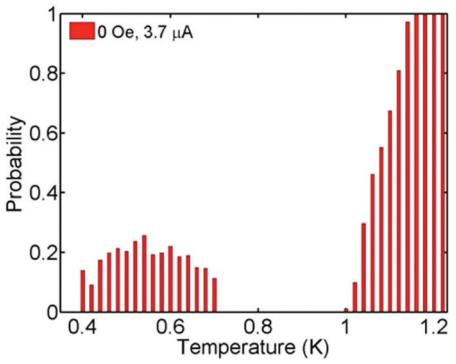

FIG. 7. (Color online) Probability of the normal state as a function of temperature for sample 2. Probability of finding the normal state in a particular measurement as a function of temperature at 0 Oe and 3.7 μA.

the switching close to T_c is different from the switching at low temperatures. The dependence of the switching probability of a superconducting nanowire in the QPS regime has been explored in a recent experiment on $Mo_{76}Ge_{24}$ nanowires, and the exponent for the dependence has been determined to be 1[27]. The switching probability dependence on current at 0.2 and 0.5 K can be seen in Figs. 6(a) and 6(b). Although there are not enough data points to extract an exponent, a nonlinearly increasing probability consistent with expectations is apparent especially in the 0.5 K plot [Fig. 6(b)].

The difference in temperature dependence of switching probability between the two regimes becomes clearer if we examine P_N as a function of temperature (Fig. 7). One very important feature of QPS in comparison to TAPS is the absence of temperature dependence in the former. If we plot the calculated switching probability as a function of temperature, it is clear that in the low-temperature QPS region, P_N has no systematic dependence on temperature, whereas near $T \sim T_c$ in the TAPS region P_N increases with temperature.

V. DISCUSSION

One may wonder if the phenomenon we have reported can be a consequence of electromagnetic noise on the nanowire. We have shown that there exists a region of intermediate temperature where the AlNW is always superconducting with no switching events that is sandwiched between the high-temperature TAPS and low-temperature QPS regions. The boundaries of these regions show a systematic dependence on the magnetic field and excitation current that is consistent with the Caldeira-Leggett mechanism. It is difficult to imagine a scenario where random electromagnetic noise can produce such a magnetic field and current dependent switching free region. Moreover, in the original experiment reporting the APE in zinc nanowires,[32] the introduction of additional low pass filters at both low and room temperatures made no difference in the results. This result also shows that APE is not a consequence of electromagnetic noise.

Another possibility is that the change in thermal conductivity of the electrodes at their superconducting transition changes how well the wire is thermalized. With superconducting electrodes, the heat generated due to phase slips in the wire cannot be dissipated away easily, and therefore, the wire is driven normal. The possibility of the antiproximity effect thus being caused by heating has been addressed and proven to be unfounded in previous publications on the subject.[34,35] In addition, the fact that the effect does not appear in low-resistivity nanowires (Fig. S4)[45] is helpful in eliminating this possibility. The low-resistivity nanowires are better thermally coupled to the electrodes and should respond to the exponential change in the thermal conductivity of the electrodes much more than the high-resistivity nanowires. Finally, estimates of heat dissipation through various channels show that, in the wires showing APE, the major channel of heat dissipation, accounting for ~90% of the heat dissipation, is through the substrate and not through the electrodes (Fig. S5).[45] With these facts in mind, we believe that the thermal conductivity change explanation can be ruled out.

Understanding the APE in terms of the QPS mechanism described above also helps solving some of the puzzles in the early experiments. One aspect it helps to understand is why the APE is only seen at certain currents.[33] In nanowires of these dimensions, the probability of quantum phase slips is very low at low-excitation currents. This probability increases exponentially with current, and the APE therefore manifests only close to the critical currents of such samples. Another aspect it clarifies is the electrode-material dependence of the APE. In Zn nanowires contacted with different electrodes, the strength of the APE was found to vary with electrode material.[32] From the QPS point of view, we can see that the current density of the measurement is the critical parameter affecting the strength of the APE and not the electrode material.

VI. CONCLUSION

In conclusion, MQT events in a simple superconducting nanowire, free from interference from classical effects, have been observed. This is possible because the Caldeira-Leggett mechanism provides a clear phase slip free region separating the QPS and TAPS regions. In these current-biased nanowires, a single quantum phase slip event makes the nanowire switch from the superconducting to the normal state. A new technique using individual resistance measurements is used to confirm the stochastic nature of the phase slip events. This is experimentally an easily detectable event and opens up possibilities for quantitative studies of individual QPS events. Moreover, these results bring forth a complete understanding of the counterintuitive APE as an experimental manifestation of the Caldeira-Leggett mechanism and resolve a number of puzzles in the early experiments.[32–35]

ACKNOWLEDGMENTS

We gratefully acknowledge informative discussions with Jainendra Jain, Chaoxing Liu, Thomas Mallouk, Mingliang Tian, and Jian Wang. This work was supported by the Penn State MRSEC under NSF Grant DMR-0820404 and the Pennsylvania State University Materials Research Institute Nano Fabrication Network and the National Science Foundation Cooperative Agreement No. 0335765, National Nanotechnology Infrastructure Network, with Cornell University.

[1] W. A. Little, Phys. Rev. **156**, 396 (1967).
[2] J. Langer and V. Ambegaokar, Phys. Rev. **164**, 498 (1967).
[3] D. McCumber and B. Halperin, Phys. Rev. B **1**, 1054 (1970).
[4] J. E. Lukens, R. Warburton, and W. Webb, Phys. Rev. Lett. **25**, 1180 (1970).
[5] M. Tian, J. Wang, J. S. Kurtz, Y. Liu, M. H. W. Chan, T. S. Mayer, and T. E. Mallouk, Phys. Rev. B **71**, 104521 (2005).
[6] A. J. Leggett, Suppl. Prog. Theor. Phys. **69**, 80 (1980).
[7] J. M. Martinis, M. H. Devoret, and J. Clarke, Phys. Rev. B **35**, 4682 (1987).
[8] G.-H. Lee, D. Jeong, J.-H. Choi, Y.-J. Doh, and H.-J. Lee, Phys. Rev. Lett. **107**, 146605 (2011).
[9] H. F. Yu, X. B. Zhu, Z. H. Peng, Y. Tian, D. J. Cui, G. H. Chen, D. N. Zheng, X. N. Jing, L. Lu, S. P. Zhao, and S. Han, Phys. Rev. Lett. **107**, 067004 (2011).
[10] L. D. Jackel, J. P. Gordon, E. L. Hu, R. E. Howard, L. A. Fetter, D. M. Tennant, R. W. Epworth, and J. Kurkijarvi, Phys. Rev. Lett. **47**, 697 (1981).
[11] J. Kurkijarvi, in *Proceedings of the Second International Conference on Superconducting Quantum Devices*, edited by H. D. Hahlbohm and H. Lubbig (deGruyter, Berlin, 1980), p. 247.
[12] J. Kurkijarvi, Phys. Rev. B **6**, 832 (1972).
[13] O. V. Astafiev, L. B. Ioffe, S. Kafanov, Y. A. Pashkin, K. Y. Arutyunov, D. Shahar, O. Cohen, and J. S. Tsai, Nature **484**, 355 (2012).
[14] J. E. Mooij and Y. V. Nazarov, Nature Physics **2**, 169 (2006).
[15] A. D. Zaikin, D. S. Golubev, A. van Otterlo, and G. T. Zimányi, Phys. Rev. Lett. **78**, 1552 (1997).
[16] M. Tinkham and C. N. Lau, Appl. Phys. Lett. **80**, 2946 (2002).
[17] N. Giordano, Phys. Rev. Lett. **61**, 2137 (1988).
[18] C. N. Lau, N. Markovic, M. Bockrath, A. Bezryadin, and M. Tinkham, Phys. Rev. Lett. **87**, 217003 (2001).
[19] A. Bezryadin, C. Lau, and M. Tinkham, Nature **404**, 971 (2000).
[20] A. Bezryadin, J. Phys.: Condens. Matter **20**, 043202 (2008).
[21] J. S. Lehtinen, T. Sajavaara, K. Y. Arutyunov, M. Y. Presnjakov, and A. L. Vasiliev, Phys. Rev. B **85**, 094508 (2012).
[22] F. Sharifi, A. V. Herzog, and R. C. Dynes, Phys. Rev. Lett. **71**, 428 (1993).
[23] M. Zgirski and K. Y. Arutyunov, Phys. Rev. B **75**, 172509 (2007).
[24] M. Sahu, M.-H. Bae, A. Rogachev, D. Pekker, T.-C. Wei, N. Shah, P. M. Goldbart, and A. Bezryadin, Nature Physics **5**, 503 (2009).
[25] M. Zgirski, K.-P. Riikonen, V. Touboltsev, and K. Arutyunov, Phys. Rev. B **77**, 054508 (2008).
[26] F. Altomare, A. M. Chang, M. R. Melloch, Y. Hong, and C. W. Tu, Phys. Rev. Lett. **97**, 017001 (2006).
[27] T. Aref, A. Levchenko, V. Vakaryuk, and A. Bezryadin, Phys. Rev. B **86**, 024507 (2012).
[28] A. T. Bollinger, A. Rogachev, and A. Bezryadin, Europhys. Lett. **76**, 505 (2006).
[29] N. Shah, D. Pekker, and P. M. Goldbart, Phys. Rev. Lett. **101**, 207001 (2008).
[30] D. Pekker, N. Shah, M. Sahu, A. Bezryadin, and P. M. Goldbart, Phys. Rev. B **80**, 214525 (2009).
[31] P. Li, P. M. Wu, Y. Bomze, I. V. Borzenets, G. Finkelstein, and A. M. Chang, Phys. Rev. Lett. **107**, 137004 (2011).
[32] M. Tian, N. Kumar, S. Xu, J. Wang, J. S. Kurtz, and M. H. W. Chan, Phys. Rev. Lett. **95**, 076802 (2005).
[33] M. Tian, N. Kumar, J. Wang, S. Xu, and M. H. W. Chan, Phys. Rev. B **74**, 014515 (2006).
[34] Y. Chen, S. D. Snyder, and A. M. Goldman, Phys. Rev. Lett. **103**, 127002 (2009).
[35] Y. Chen, Y. H. Lin, S. D. Snyder, and A. M. Goldman, Phys. Rev. B **83**, 054505 (2011).
[36] M. Singh, J. Wang, M. Tian, T. E. Mallouk, and M. H. W. Chan, Phys. Rev. B **83**, 220506(R) (2011).
[37] A. O. Caldeira and A. J. Leggett, Phys. Rev. Lett. **46**, 211 (1981).
[38] S. Chakravarty, Phys. Rev. Lett. **49**, 681 (1982).
[39] A. J. Leggett, S. Chakravarty, A. Dorsey, M. Fisher, A. Garg, and W. Zwerger, Rev. Mod. Phys. **59**, 1 (1987).
[40] H. C. Fu, A. Seidel, J. Clarke, D.-H. Lee, Phys. Rev. Lett. **96**, 157005 (2006).
[41] D. B. Schwartz, B. Sen, C. N. Archie, and J. E. Lukens, Phys. Rev. Lett. **55**, 1547 (1985).
[42] A. N. Cleland, J. M. Martinis, and J. Clarke, Phys. Rev. B **37**, 5950 (1988).
[43] B. Abeles, R. Cohen, and G. Cullen, Phys. Rev. Lett. **17**, 632 (1966).
[44] G. Deutscher, H. Fenichel, M. Gershenson, E. Grünbaum, and Z. Ovadyahu, J. Low Temp. Phys. **10**, 231 (1973).
[45] See Supplemental Material at http://link.aps.org/supplemental/10.1103/PhysRevB.88.064511 for detailed experimental methodology, additional experimental results, and heat flow calculations.
[46] M. Tian, J. Wang, J. Snyder, J. Kurtz, Y. Liu, P. Schiffer, T. E. Mallouk, and M. H. W. Chan, Appl. Phys. Lett. **83**, 1620 (2003).
[47] V. L. Ginzburg, Phys. Lett. **13**, 101 (1964).
[48] A. A. Shanenko, M. D. Croitoru, M. Zgirski, F. M. Peeters, and K. Arutyunov, Phys. Rev. B **74**, 052502 (2006).
[49] P. Xiong, A. V. Herzog, and R. C. Dynes, Phys. Rev. Lett. **78**, 927 (1997).
[50] D. Y. Vodolazov, D. S. Golubović, F. M. Peeters, and V. V. Moshchalkov, Phys. Rev. B **76**, 134505 (2007).
[51] D. Y. Vodolazov, Phys. Rev. B **75**, 184517 (2007).
[52] M. Tinkham, *Introduction to Superconductivity*, Dover Edit (Dover Publications, Mineola, 2004).
[53] E. Swartz and R. Pohl, Rev. Mod. Phys. **61**, 605 (1989).
[54] P. Li, P. M. Wu, Y. Bomze, I. V. Borzenets, G. Finkelstein, and A. M. Chang, Phys. Rev. B **84**, 184508 (2011).
[55] J. S. Kurtz, R. R. Johnson, M. Tian, N. Kumar, Z. Ma, S. Xu, and M. H. W. Chan, Phys. Rev. Lett. **98**, 247001 (2007).
[56] N. Phillips, Phys. Rev. **114**, 676 (1959).
[57] C. Satterthwaite, Phys. Rev. **125**, 873 (1962).
[58] S. Sahling, J. Engert, A. Gladun, and R. Knoner, J. Low Temp. Phys. **45**, 457 (1981).
[59] P. Mohanty, D. A. Harrington, K. L. Ekinci, Y. T. Yang, M. J. Murphy, and M. L. Roukes, Phys. Rev. B **66**, 085416 (2002).
[60] T. Jeong, J.-G. Zhu, S. Chung, and M. R. Gibbons, J. Appl. Phys. **111**, 083510 (2012).